



Honors College Theses


---

12-15-2022

## Nanoparticle conjugated photosensitizer for targeted photodynamic inactivation of cancer cells

Symone D. Crowder  
*Georgia Southern University*

Follow this and additional works at: <https://digitalcommons.georgiasouthern.edu/honors-theses>

 Part of the [Biochemistry Commons](#), [Biotechnology Commons](#), [Medicinal Chemistry and Pharmaceutics Commons](#), and the [Medicine and Health Sciences Commons](#)

---

### Recommended Citation

Crowder, Symone D., "Nanoparticle conjugated photosensitizer for targeted photodynamic inactivation of cancer cells" (2022). *Honors College Theses*. 811.  
<https://digitalcommons.georgiasouthern.edu/honors-theses/811>

This thesis (open access) is brought to you for free and open access by Digital Commons@Georgia Southern. It has been accepted for inclusion in Honors College Theses by an authorized administrator of Digital Commons@Georgia Southern. For more information, please contact [digitalcommons@georgiasouthern.edu](mailto:digitalcommons@georgiasouthern.edu).

***Nanoparticle conjugated photosensitizer for targeted photodynamic inactivation of cancer cells***

An Honors Thesis submitted in partial fulfillment of the requirements for Honors in the  
*Department of Chemistry and Biochemistry*

By

*Symone Crowder*

Under the mentorship of *Dr. Ria Ramoutar & Dr. Debanjana Ghosh*

**ABSTRACT**

*Photodynamic therapy (PDT) is considered to be a potential replacement for traditional methods of chemotherapy. It includes the administration of photosensitizing agents (PS), which generate reactive oxygen species (ROS) upon excitation at a specific wavelength. With new outlooks and techniques, cancer research is advancing each day. It has allowed the progress of several theranostic drug delivery systems (DDS) exploring the area of nanomedicine.<sup>2</sup> In the present work, a Rhodamine derivative, Rhodamine 6G (R6G) was used as the PS. In general, rhodamine compounds undergo cytotoxic reactions on photoexcitation by electron transfer reactions with folic acid within cells, making them a favorable PS. However, rhodamines often experience poor water solubility which limits their applications in biological environments. Additionally, the process of PDT requires a high accumulation of photosensitizers. To overcome the challenge of aqueous compatibility of rhodamine compounds as well as retaining its specific functioning in cells at a reduced optimum concentration, this project focused on developing a nanocarrier system using gold nanoparticles (GNPs) to help deliver those dyes to the cancer targets. The GNPs were synthesized with a particle size ranging from 16 to 30 nm. Towards the aim to understand the photodynamic inactivation of cancer cells, absorption and fluorescence spectroscopic techniques were utilized. Dynamic Light Scattering (DLS) spectroscopy has been used to measure the hydrodynamic size of the nanoparticles. UV-Vis and fluorescence spectroscopy analyzed the nanocomposite with the rhodamine derivative and studied the immobilization over time. The 24-hour experiments provided a route for GNP conjugated rhodamine dye towards using PDT as the most viable method.*

Thesis Mentor: *Dr. Debanjana Ghosh*

Honors Dean: *Dr. Steven Engel*

December 2022

*Department of Chemistry and Biochemistry*

Honors College

**Georgia Southern University**

### **Acknowledgements:**

This project would not have been possible without the help of the wonderful programs and faculty of Georgia Southern University. To begin, Dr. Shainaz Landge, who saw potential in me and encouraged me to start research, and Dr. Debanjana Ghosh, who took me on as her student. These two also encouraged me to apply to the McNair scholars program and wrote letters of recommendation on my behalf. The McNair Scholars program has opened a world of possibilities to me, supporting me through two summer research experiences and three conference presentations, each of which has helped me grow as a researcher, student, and individual. One cornerstone of each summer research experience has been Dr. Ria Ramoutar, who has served as a mentor and source of encouragement to me far before she was kind enough to take me on as a research student as well. Finally, I would like to thank the College of Science and Mathematics at Georgia Southern University for selecting me as a recipient of the COUR grant. Without each of these influences, the present work would not have been possible.

I sincerely thank each and every organization and individual who has helped me to complete this journey.

## 1. Introduction

When it comes to treating cancer, the process is synonymous with chemotherapy, radiation, and a taxing battle that could cause severe detriment to the patient long before they get better. Chemotherapy in combination with radiation was first used as a treatment option in the 1940's<sup>8</sup>, but the substantial effects the treatment has on the healthy cells of the body, as well as the limitations the treatment has with late-stage cancers has always left the door open to research new methods of treatment. In the years since then, different efforts have been focused on cancer vaccines as well as drugs that diffuse into cancerous cells. Photodynamic therapy (PDT) is an additional prospect that hopes to one day allow for the phasing-out of chemotherapy and radiation as the primary option for cancer treatment.

The name "Photodynamic therapy" itself was first coined by the German scientist and professor Herman Von Tappeiner in the year 1907. The word was then used to describe the effect that the presence or absence of light had on "oxygen-dependent photosensitization".<sup>2</sup> While the field of what would now be considered "phototherapy" dates back all the way to the ancient Egyptians,<sup>2</sup> the discovery of photodynamic therapy itself was somewhat of an accident. Oscar Raab, a student of Von Tappeiner's, was tasked with studying the effects of an acridine chemical against malaria samples when he noted that what marked the change in the effectiveness of the chemical was higher on the day that a thunderstorm had caused drastically different light conditions for the experiment.<sup>2</sup> This theory was expanded upon until they proved conclusively that light had an advantageous effect on the acridine chemical, and further that it was not the light itself, but the effects of fluorescence within biological systems.<sup>2</sup> The study concluded with the

incomplete hypothesis that there was a transfer of energy from light to chemical, similar to photosynthesis, which increased the effectiveness of the drug.<sup>2</sup> Von Tappeiner himself furthered this theory with use of the photosensitizer, eosin, for the treatment of skin cancer, concluding that this process also needed oxygen.<sup>2</sup> This discovery brought together all of the pieces to define photodynamic therapy as it is still known to this day.

The necessity of oxygen presence for photodynamic therapy comes from the nature of fluorescence itself. Fluorescence is observed when the correct wavelength of light causes a stable molecule to enter an excited state. A short period of excitation is known as a singlet state, while a longer excitation time is known as the triplet state. This triplet state is where the excited molecule becomes the “photo-active species,” which interacts with an oxygen molecule to produce singlet oxygen. Singlet oxygen leads to photo-oxidation within a cell, eventually leading to the cell’s death.

Modern advancements in photodynamic therapy have begun utilizing nanoparticles coated by photosensitizer drugs. The photosensitizer drugs used in this scenario serve three functions. They first increase the solubility of nanoparticles in water, allowing for greater passage of the solution through the body. Second, photosensitizer drugs allow the nanoparticles to accumulate within cancerous cells so that they may be targeted independently of healthy cells. Finally, they determine the required wavelength for the light which will be used to excite the nanoparticles. This excitation may also be used to cause the nanoparticles within the cancerous mass or cancer cells to generate heat, causing the cancerous cells to die via photothermal therapy.<sup>11</sup> Photodynamic therapy, in contrast, is dependent on the formation of reactive oxygen species (ROS). PDT has yet to be used in a large-scale capacity, with one aspect preventing the widespread use of Gold Nanoparticles

(GNPs) for photodynamic therapy being the unknown time frame of viability for synthesized GNPs.

The present work synthesizes GNPs for subsequent incubation with photosensitizer, Rhodamine 6G (R6G), in order to establish a timeline of viability for nanoparticle-conjugated photosensitizers. Knowing these parameters will help photodynamic therapy become a more plausible option within an industry or hospital setting, bringing the field even closer to public use.

In literature, methods for the sizing of gold nanoparticles based on their UV-Visible (UV-Vis) absorbance have been established.<sup>4</sup> PDT itself can utilize absorbances in both the IR and “Near IR” region on the electromagnetic spectrum.<sup>9</sup> Throughout this project, UV-Vis is used extensively in accordance with this. Both size estimations and capability for photodynamic therapy were established this way, culminating in the incubation study wherein it was found that gold nanoparticles when combined with photosensitizer remain viable for approximately 48 hours.

## **2. Materials:**

### Chemicals Used:

Gold (III) chloride was purchased from Sigma Aldrich. Trisodium citrate dihydrate was purchased from Spectrum Chemical Corporation. Deionized (DI) water from filtered and collected in-lab. Rhodamine 6G purchased from Acros Organics.

### Instruments Used:

Thermo Fisher scientific Epure water filtration system, Shimadzu UV-2600 UV-Vis Spectrophotometer, Perkin Elmer LS 55 Fluorescence Spectrometer, Malvern Nano-

Zs Zetasizer, JEOL JSM-7600 F Field Emission Scanning Electron Microscope.

### **3. Methods:**

#### **Synthesis of Gold Nanoparticles (GNPs)**

GNPs were synthesized using methods established in published literature.<sup>4</sup> 500  $\mu$ L of  $3.37 \times 10^{-2}$  M HAuCl<sub>4</sub> were added to a 100 mL round bottom flask containing 50 g deionized (DI) water. The solution was placed on a hot plate on high heat and allowed to stir until boiling. Next, 1 mL of  $3.54 \times 10^{-2}$  M trisodium citrate solution was added to the boiling solution. Upon color change, the heat was turned off and the solution was allowed to stir until cool.

#### **Combination of GNP with Rhodamine 6G for incubation**

The rhodamine 6G (R6G) photosynthesizer was used for incubation in concentrations ranging from  $1.67 \times 10^{-7}$  M R6G in GNP to  $1.67 \times 10^{-5}$  M R6G in GNP. These concentrations were  $1.67 \times 10^{-7}$  M R6G in GNP,  $5.00 \times 10^{-7}$  M R6G in GNP,  $1.67 \times 10^{-6}$  M R6G in GNP,  $3.33 \times 10^{-6}$  M R6G in GNP,  $8.33 \times 10^{-6}$  M R6G in GNP, and  $1.67 \times 10^{-6}$  M R6G in GNP. Control data was also collected at these same concentrations for R6G in water. Each solution was made just before subsequent UV-Vis or fluorescence spectroscopies were collected in order to ensure the least time possible between creation and the “initial” measurement of each sample. Subsequent incubation times were then based on each individual time of combination with R6G.

#### **UV-Vis and Fluorescence Spectroscopies**

UV-Vis data was collected using a Shimadzu UV-2600 UV-Vis Spectrophotometer to obtain absorption spectra for each sample from 200-900 nm.

Fluorescence spectroscopy was conducted on a Perkin Elmer LS 55 Fluorescence Spectrometer. The excitation wavelength was set as 526 nm, corresponding to Rhodamine 6G's  $\lambda_{\text{max}}$ .<sup>13</sup> The excitation slit was set as 5 nm and the emission slit was set as 2.5 nm, with the spectra being collected on the interval 531-750 nm.

When performed in tandem, UV-Vis and fluorescence spectra were taken in alternation with each other, ensuring that the initial measurements, as well as all subsequent incubation readings were as accurate as possible.

#### **Characterization of GNP Solution by Dynamic Light Scattering**

Dynamic Light Scattering (DLS) was used to characterize the approximate size of nanoparticles within solution. DLS operates on the principle of Rayleigh light scattering through a solution with suspended spherical particles to measure the diameter of particles smaller than the wavelength of visible light.<sup>7</sup> This principle makes DLS a great technique for the characterization of the spherical nanometer-sized samples synthesized in this project. For DLS measurements, approximately 10 mL of GNP sample (without R6G) was centrifuged and subsequently filtered through a 0.2  $\mu\text{m}$  microfilter, from which a 1 mL sample was tested. Each DLS solution was set to run in three trials, creating 9 graphs per sample and 3 error source reports for a total of 12 graphs per GNP solution. All data was collected using a Malvern Nano-Zs Zetasizer.

#### **4. Results and Discussion:**

##### **Characterization of synthesized Gold Nanoparticles (GNPs)**

The GNPs synthesized following the methods described in Section 3 were characterized using steady-state UV-Vis spectroscopy. The characteristic surface plasmon



resonance spectrum profile for spherical nanometals is depicted in Figure 1a-c with absorption band maxima or wavelengths ( $\lambda_{\max}$ ) in the range of 518 – 524 nm. [4]

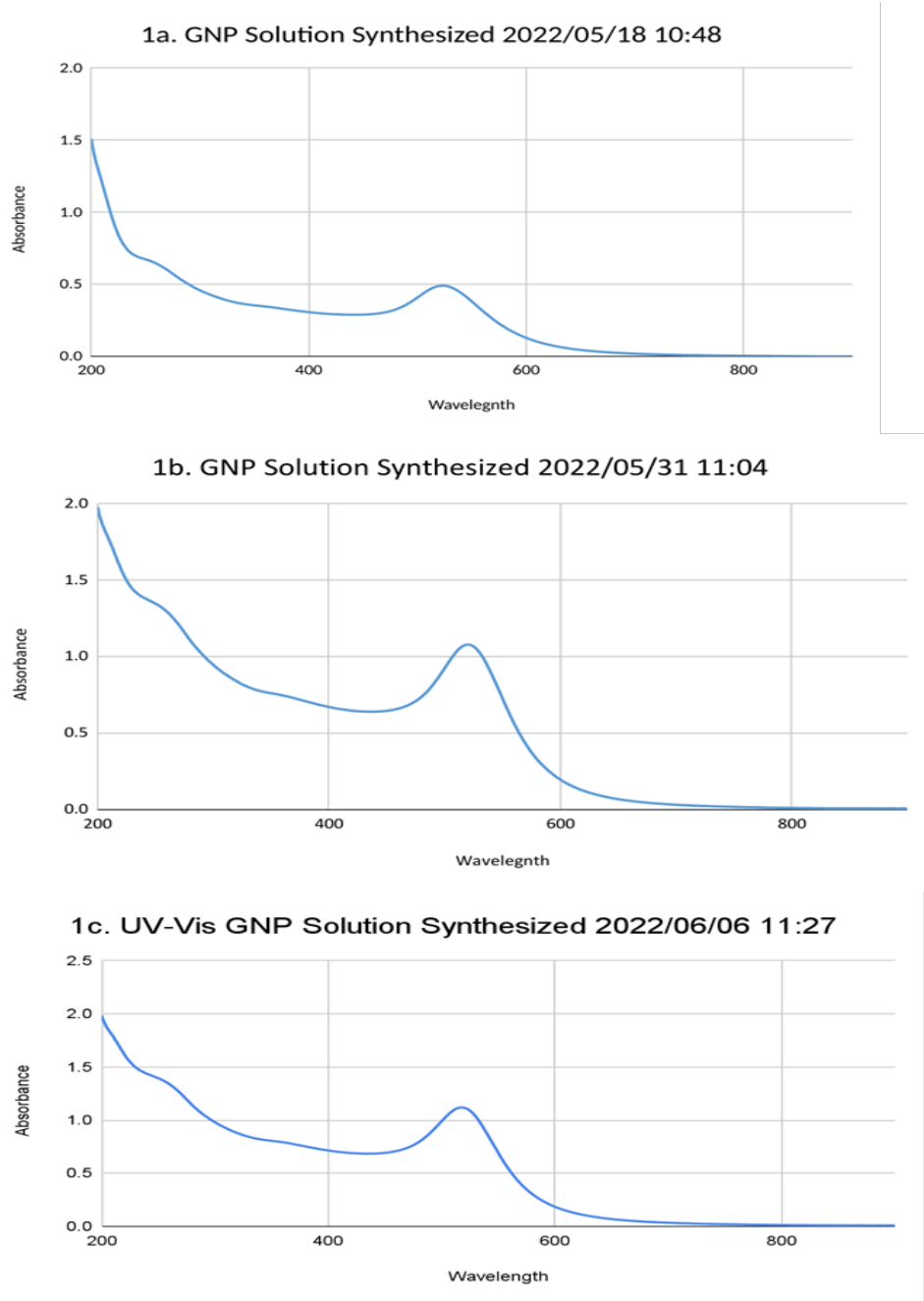


**Figure 1a-c:** Steady-state absorption spectra for the synthesized gold nanoparticles (GNPs) at (a)  $\lambda_{\max} = 524$  nm, (b)  $\lambda_{\max} = 521$  nm, and (c)  $\lambda_{\max} = 518$  nm.

Figure 2a-c shows the reddish color indicative of GNP synthesized within these wavelengths. The variation in the  $\lambda_{\text{max}}$  depends on several factors such as the molar volume or the mole fraction of citrate added or the time at which the citrate salt is added while the acid was stirring at a boiling temperature.

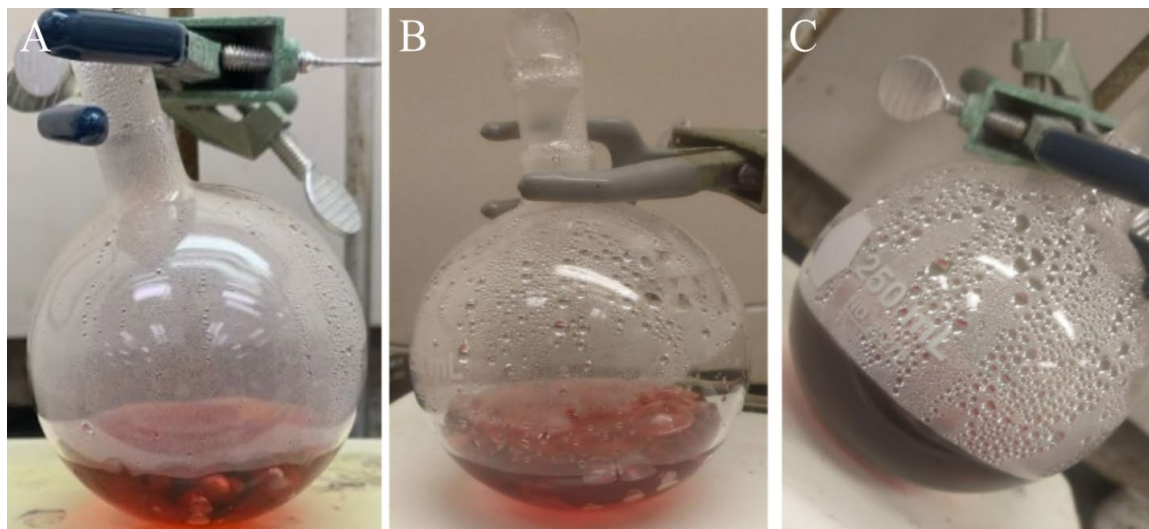
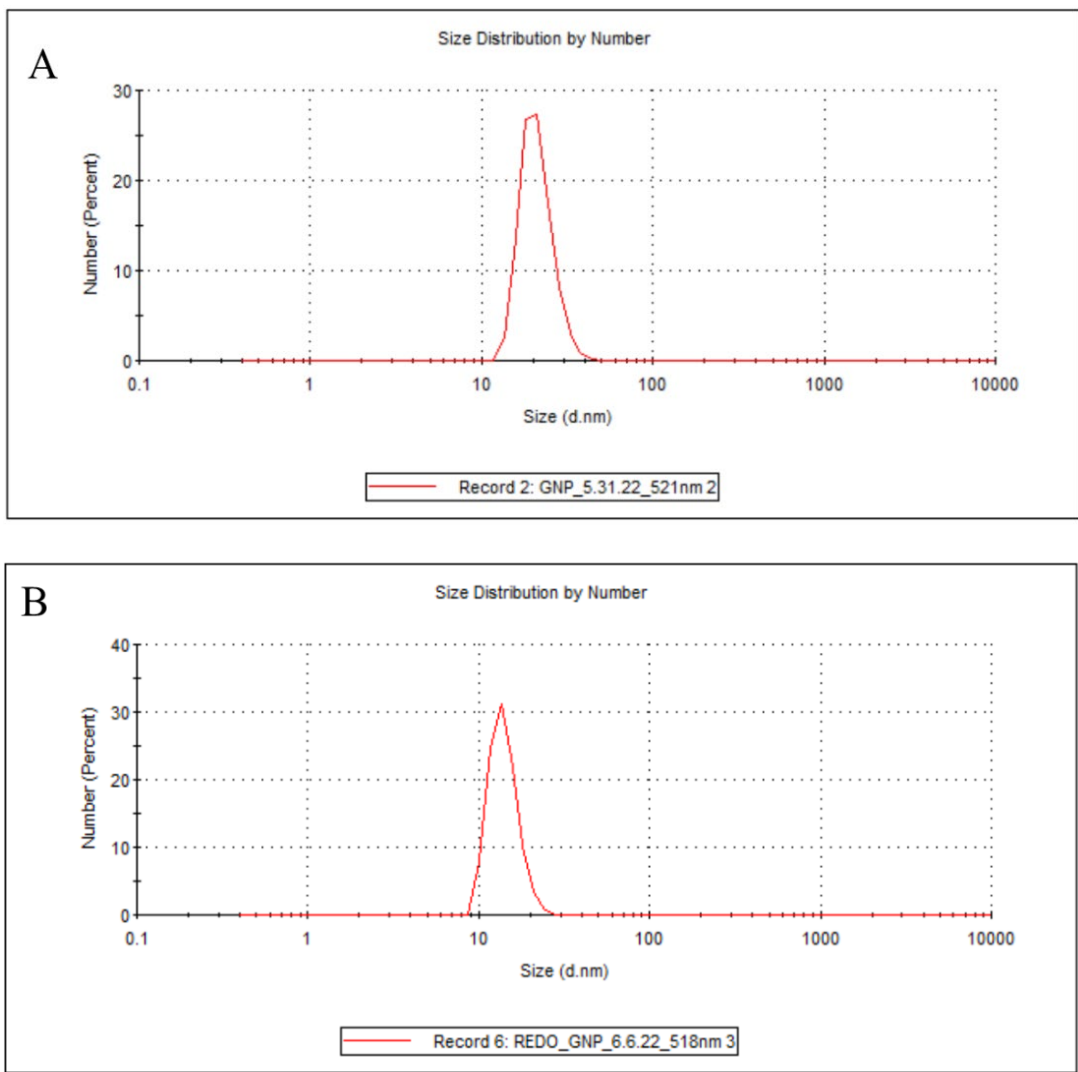


**Figure 2 a-c:** The reddish colors for the characteristic UV-Vis spectra band maxima for various synthesized GNPs.

The *estimated* diameter of GNPs can be determined using  $\lambda_{\text{max}}$  from the absorption spectra and the equation  $Y = 2.99 X - 1539$ , where Y is the GNP diameter in nanometers (nm) and X refers to  $\lambda_{\text{max}}$  in nm. The equation is based on a standard linear plot showing the correlation between the estimated GNP diameter from Transmission Electron Microscopy (TEM) measurements and band maxima data obtained from UV-Vis as reported by Ghosh *et al.*<sup>4</sup> Based on this equation, the particle size (diameter) for our synthesized GNPs is estimated to be approximately 27.76 nm for the sample with a  $\lambda_{\text{max}}$  of 524 nm, 18.79 nm for  $\lambda_{\text{max}}$  of 521 nm and 9.82 nm for  $\lambda_{\text{max}}$  of 518 nm.

The synthesized GNPs were then characterized through Dynamic Light Scattering (DLS) technique to more accurately determine their hydrodynamic particle size. Figure 3a-

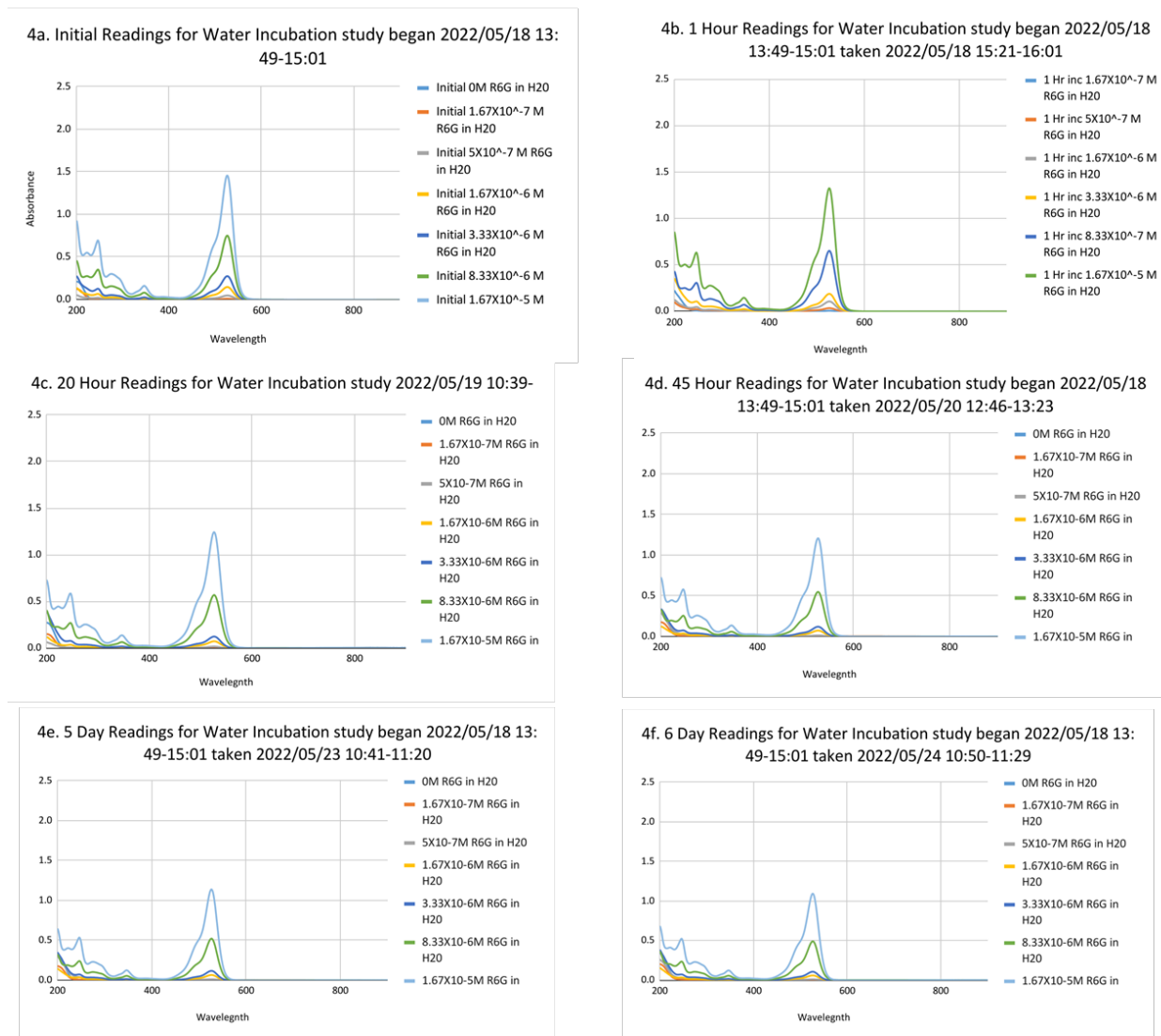
b shows the size distribution spectra for two GNP samples. The GNP sample with absorption maximum band at 521 nm has an average diameter of  $\sim 21$  nm (Figure 3a) while the sample with  $\lambda_{\max}$  at 518 nm is  $\sim 14$  nm and (Figure 3b). While these DLS measurements are more accurate, they are relatively comparable to the particle sizes estimated earlier through UV-Vis. The particle sizes as indicated by DLS are in correlations to the previously published works<sup>4,13</sup> and corroborates that the shorter the  $\lambda_{\max}$  the smaller the particle size.



**Figure 3a-b:** Size distribution of GNP solutions with  $\lambda_{\max}$  at (a) 521 nm and (b) 518 nm. All measurements were taken using Malvern Nano-Zs Zetasizer.

## Exploring the photosensitizer (PS), Rhodamine 6G (R6G)

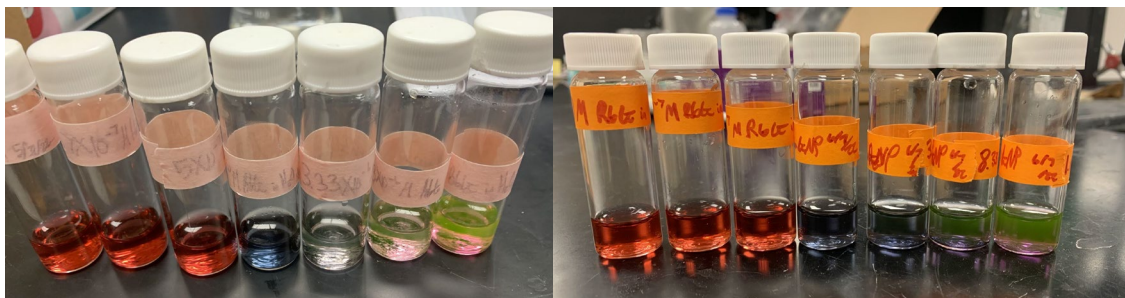
To understand the efficiency of R6G in nanoparticle conjugate drug delivery, the photosensitizing effect of the molecule was studied through a series of incubations in GNPs. It is important to determine the stability of R6G in the absence of GNP in order to compare and understand its effectiveness as a photosensitizer upon GNP conjugation.



**Figure 4a-f:** UV-Vis spectra for the control, R6G in in DI water at various concentrations and time. R6G concentrations are  $1.67 \times 10^{-7}$  M,  $5.00 \times 10^{-7}$  M,  $1.67 \times 10^{-6}$  M R6G,  $3.33 \times 10^{-6}$  M R6G,  $8.33 \times 10^{-6}$  M, and  $1.67 \times 10^{-6}$  M, respectively. Incubation times are 0 hours (initial), 1 hour, 20 hours, 45 hours, 5 days, and 6 days, respectively. Wavelength is in nm.

Figures 4a-4f show the control data (R6G in DI water only) taken at the same R6G concentrations and time used for the photosensitizer-gold nanoparticle conjugates the incubation time study. The data show that independent of PS concentration or incubation time, R6G is stable as indicated by its characteristic absorbance peak at 526 nm ( $\lambda_{\max}$ ).

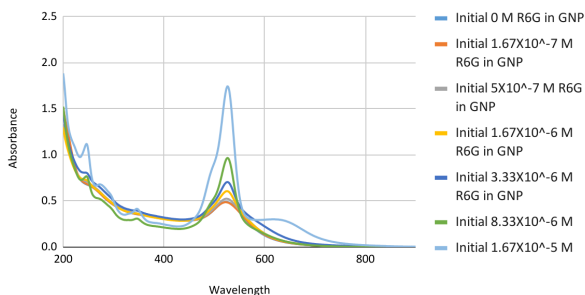
The stability of the PS is, however, altered by its conjugation with gold nanoparticle solution. This effect was studied experimentally at various R6G concentrations in GNP and incubation times using UV-Vis and fluorescence spectroscopies. Upon addition of the photosensitizer to GNP solutions, color changes are observed in the vials from the standard reddish color of the GNP solution to a blue or violet color depending on R6G concentrations as seen in Figure 5. Over time, all GNPs will aggregate and fall out of solution (black solid particles) turning the solutions clear. The color changes are in accordance with the UV-Vis analysis, which suggests a loss of viability for use in PDT.



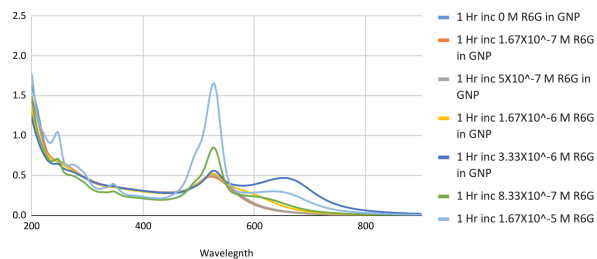
**Figure 5a-b:** Gold nanoparticle solutions during incubation study with increasing R6G concentration from left to right. 5a was captured 2022/06/06 11:00 and 5b was captured 2022/06/07 14:29.

Figure 6a-f shows the behavior of a R6G conjugated GNP solution over time. Significant absorbance shifts of particular particle solutions from their original  $\lambda_{\max}$  can be seen most prevalently in the initial reading (Figure 6a) and after 1 hour (Figure 6b), 20 hours (Figure 6c), and 45 hours (Figure 6d).

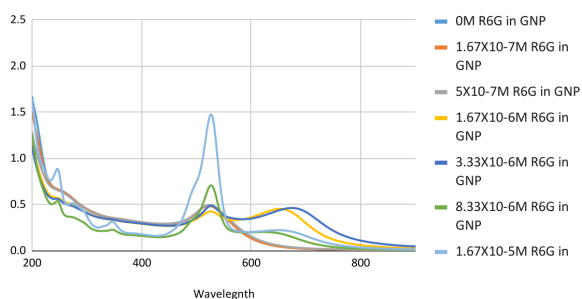
6a. Initial Readings for GNP Incubation study taken 2022/05/18 16:05-16:44



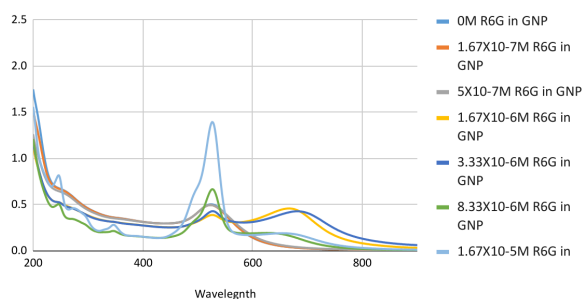
6b. 1 Hour Readings for GNP Incubation study began 2022/05/18 16:05-16:44 taken 2022/05/18 16:54-17:44



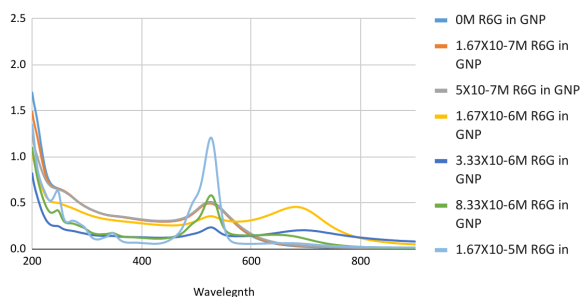
6c. 20 Hour Readings for GNP Incubation study began 2022/05/18 16:05-16:44 taken 2022/05/19 11:24-12:05



6d. 45 Hour Readings for GNP Incubation study began 2022/05/18 16:05-16:44 taken 2022/05/20 13:39-14:05



6e. 5 Day Readings for GNP Incubation study began 2022/05/18 16:05-16:44 taken 2022/05/23 11:26-12:04



6f. 6 Day Readings for GNP Incubation study began 2022/05/18 16:05-16:44 taken 2022/05/24 10:50-11:29

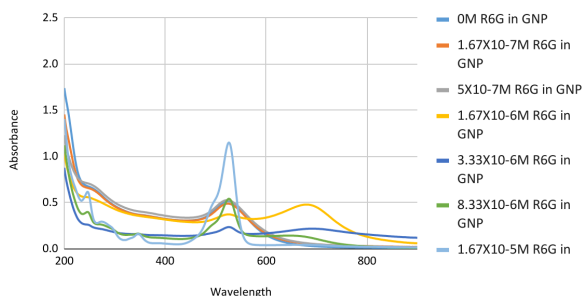


**Figure 6a-f:** UV-Vis spectra for the six-day incubation of various concentrations of R6G in GNP solution between wavelengths 200-900 nm. Peak absorbance for the GNP solution synthesized on 2022/05/18 was 524 nm indicating a particle size of 27.76 nm ( $\pm 1\%$ ) in diameter before combination with R6G.<sup>4</sup>

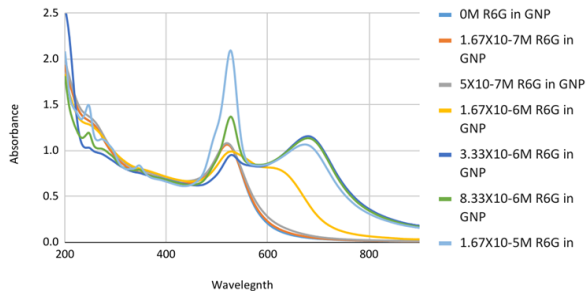
Observance of absorbance peak shifts from the initial  $\lambda_{\max}$  at 524 nm (Figure 1a) to a higher wavelength indicated the concentrations of R6G that were best suited to complex with the GNP solution. These concentrations were  $1.67 \times 10^{-6}$  M R6G in GNP and  $3.33 \times$

$10^{-6}$  M R6G in GNP. Similar peak shifts were not observed at incubation times longer than 45 hours (Figures 6e-f), which may be due to the visible precipitation of aggregated particles indicating a loss of viability. Due to these observations, subsequent incubation studies were performed between 0 and 48 hours with an absorbance reading taken every hour.

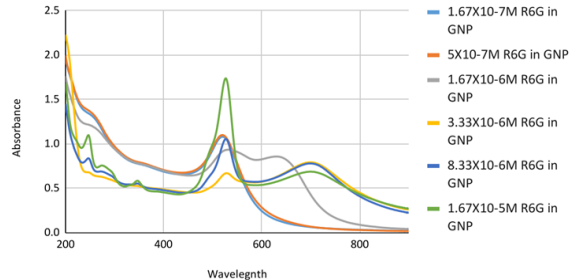
The first reduced interval incubation study was completed within the first 2 hours of mixing of R6G with GNP (Figures 7a-7c). This experiment again showed absorbance shifts in the complexes most capable of conjugating with Rhodamine 6G. This time, however, the concentrations  $1.67 \times 10^{-6}$  M R6G in GNP,  $3.33 \times 10^{-6}$  M R6G in GNP,  $8.33 \times 10^{-6}$  M R6G in GNP, and  $1.67 \times 10^{-5}$  M R6G in GNP each showed absorbance shifts (blue-shifted), however the absorbance peak was lower than the peak prior to R6G addition (i.e. GNP solution only). R6G-GNP conjugation occurs when there is a blue-shift upon addition of R6G to GNP resulting in a higher absorbance peak than that of GNP only *and* therefore a new maximum band ( $\lambda_{\max}$ ). This effect is observed for only the  $3.33 \times 10^{-6}$  M R6G in GNP solution ( $\leq 45$  hours) with its new peak absorbance at  $\lambda_{\max}$  between 680 nm to 705 nm (Figures 7a-c) rather than at 521 nm, characteristic of the GNP solution with no R6G added.

Over time ( $> 45$  hours), the appearance of a new red-shifted absorption peak is observed for  $3.33 \times 10^{-6}$  M R6G in GNP (Figures 6e-f). This change from blue to red shifted peaks indicates that the GNPs are aggregating with R6G causing the absorbance of the solution to resemble the established  $\lambda_{\max}$  in the control data (Figures 4a-f). This analysis is consistent with the color changes and precipitation of the black solid aggregates visually observed in the vials as mentioned earlier (Figure 5a-b).

7a. Initial Readings for GNP Incubation study began 2022/06/02 9:57-10:45



7b. 1 Hour Readings for GNP Incubation study began 2022/06/02 9:57-10:45 taken 2022/06/02 11:06-11:47



7c. 2 Hour Readings for GNP Incubation study began 2022/06/02 9:57-10:45 taken 2022/06/02 11:59-12:45

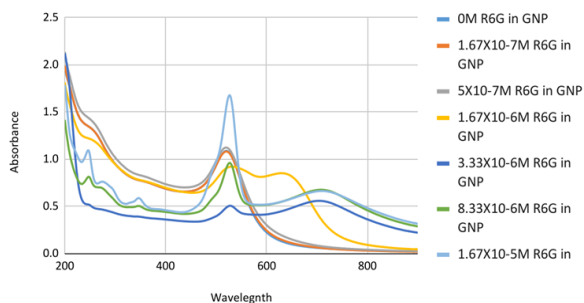


**Figure 7a-c.** Shortened incubation of R6G in GNP solution taken between wavelengths 200-900 nm. Peak absorbance for the GNP solution synthesized on 2022/05/31 and incubated on 2022/06/02 was 521 nm, indicating a particle size of 18.79 nm ( $\pm 1\%$ ) in diameter before combination with R6G.

These UV-vis readings were taken in tandem with the fluorescence spectroscopy readings shown in Figures 8a-c, which also show an absorbance shift over time. This shift in absorbance indicates that while the  $\lambda_{\text{max}}$  of the lower concentrated GNP solutions had not changed, there was still some level of conjugation occurring because of the change in peak emission of the measured samples. It should be noted that the full extent of the data cannot be seen due to the instrument detection limit. This led to the use of an alternate fluorimeter in order to continue experimentation.



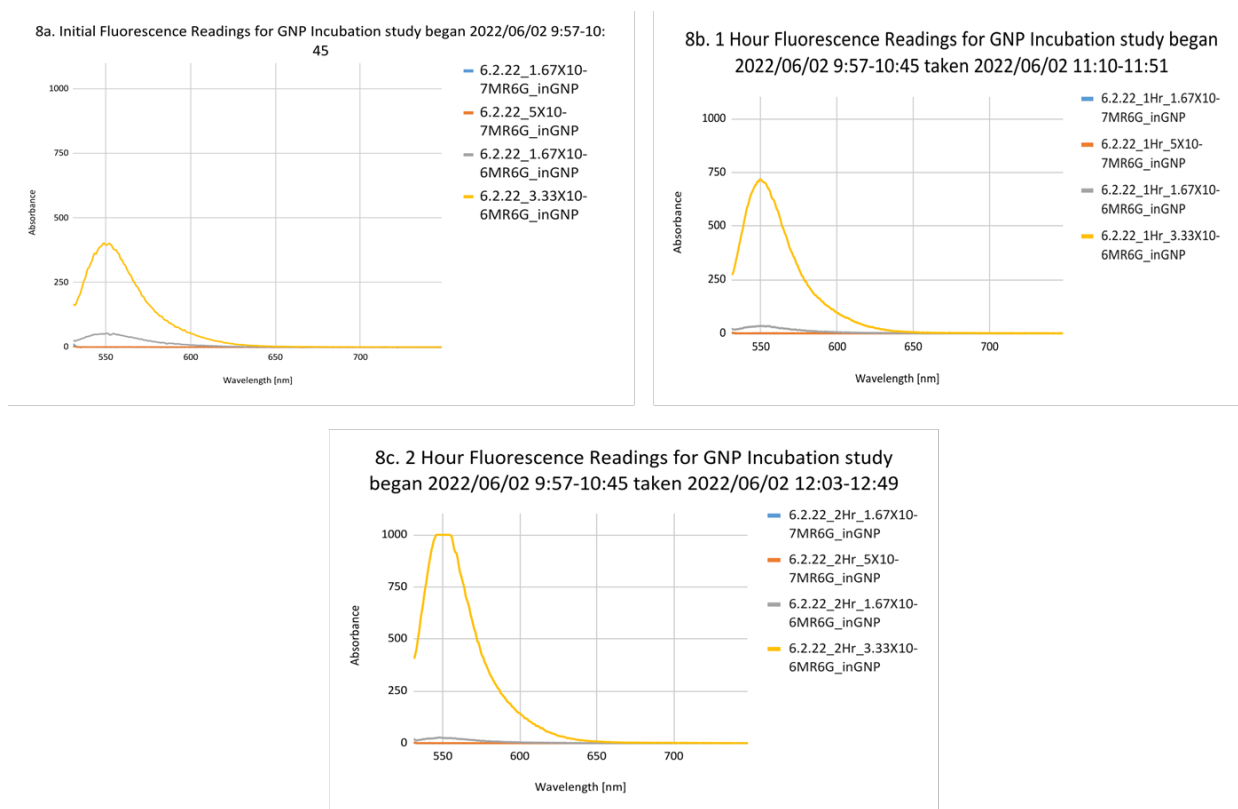


**Figure 8.** Fluorescence spectroscopy data for GNP solution synthesized on 2022/05/31, taken in tandem with the UV-Vis measurements in Figure 7.  $1.67 \times 10^{-7}$  M -  $3.33 \times 10^{-6}$  M R6G in GNP.

A similar incubation study was conducted on a GNP solution with  $\lambda_{\text{max}}$  at 518 nm (Figure 1c) and hourly time intervals up to 24 hours, seen as Figures 9a-9c. This study showed results consistent with the previous incubation study (Figures 7a-7c) with the concentrations  $1.67 \times 10^{-6}$  M R6G in GNP,  $3.33 \times 10^{-6}$  M R6G in GNP,  $8.33 \times 10^{-6}$  M R6G in GNP, and  $1.67 \times 10^{-5}$  M R6G in GNP, each showing absorbance shifts with no change in  $\lambda_{\text{max}}$ . Like before, only the  $3.33 \times 10^{-6}$  M R6G in GNP solution resulted in a true change in  $\lambda_{\text{max}}$ . The data indicates a significant absorbance decrease and aggregation increase between 2 and 24 hours, suggesting the PS-GNP conjugate may be most viable for up to two hours.

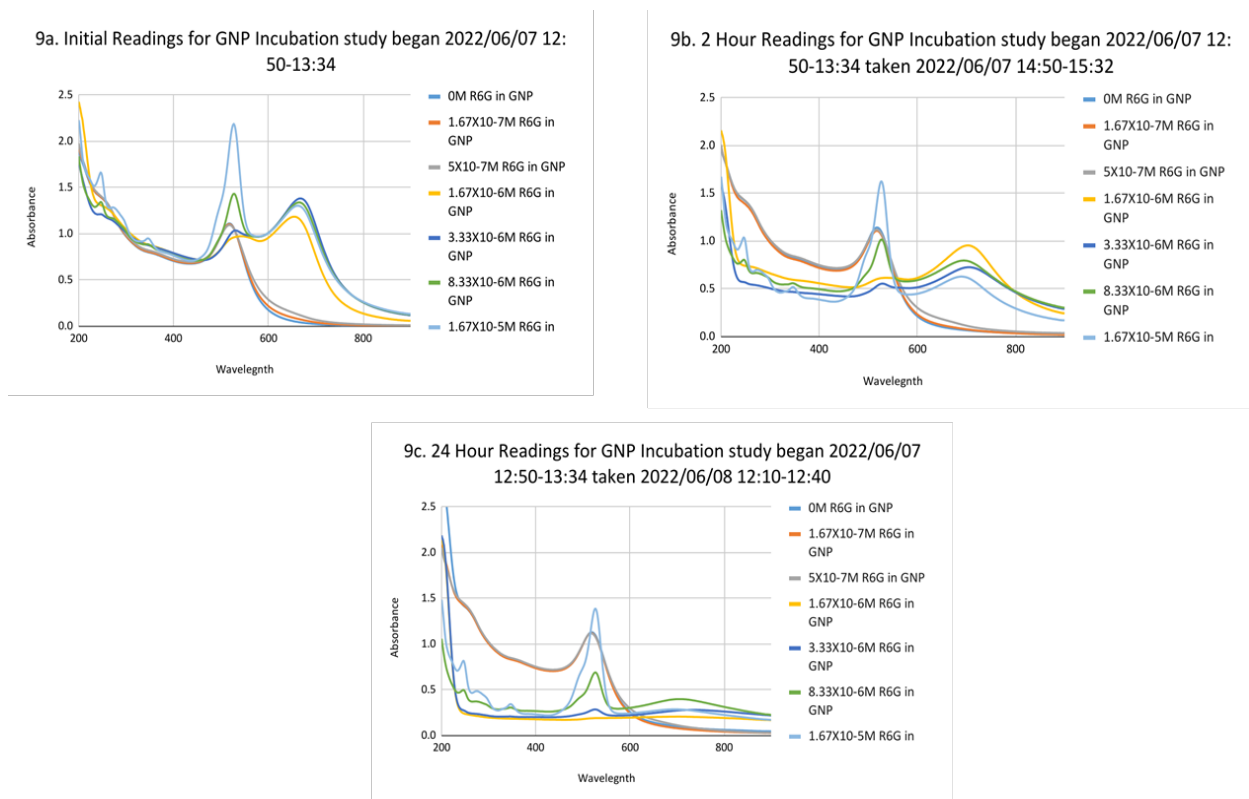


**Figure 9a-c.** Shortened incubation of R6G in GNP solution. UV-Vis measurements were taken between wavelengths 200-900 nm. This GNP solution was synthesized on 2022/06/06 had a peak absorbance at 518 nm indicating a particle size of 9.82 nm ( $\pm 1\%$ ) in diameter before combination with R6G. Incubation studies were performed on 2022/06/07.

Fluorescence incubation study for this R6G-GNP conjugate was also conducted but was inconclusive due to saturation of the data; further studies are underway on this aspect.

**Conclusion:**

Overall, we were able to synthesize GNP of diameter 16-28 nm as indicated by UV-Vis and DLS results. The small particle size enhanced the surface activity of the nanoparticles when conjugated with the photosensitizer, R6G. The steady-state absorption analysis indicated that the most effective concentration of Rhodamine 6G in GNP solution was  $3.33 \times 10^{-6}$  M. This concentration of R6G with conjugated GNP solution is only viable within the first 48 hours of R6G addition. Future studies will involve continued

fluorescence analysis on various R6G-GNP conjugates as well as TEM imaging to better determine the particle size of GNPs themselves. Analysis of the *in vivo* effects of these photosensitizer conjugate systems is necessary in order to explicate the efficacy and specificity of the established GNP conjugates in aggregating within cancerous cells towards photodynamic therapy.

### **Works Cited:**

1. Alea-Reyes, M. E.; Soriano, J.; Mora-Espí, I.; Rodrigues, M.; Russell, D. A.; Barrios, L.; Pérez-García, L. Amphiphilic Gemini Pyridinium-Mediated Incorporation of Zn(II)Meso-Tetrakis(4-Carboxyphenyl)Porphyrin into Water-Soluble Gold Nanoparticles for Photodynamic Therapy. *Colloids and Surfaces B: Biointerfaces* 2017, 158, 602–609.
2. Daniell, M. D.; Hill, J. S. A History of Photodynamic Therapy. *ANZ Journal of Surgery* 1991, 61, 340–348.
3. Gao, W.; Hu, C.-M. J.; Fang, R. H.; Luk, B. T.; Su, J.; Zhang, L. Surface Functionalization of Gold Nanoparticles with Red Blood Cell Membranes. *Advanced Materials* 2013, 25, 3549–3553.
4. Ghosh, D.; Sarkar, D.; Girigoswami, A.; Chattopadhyay, N. A fully standardized method of synthesis of gold nanoparticles of desired dimension in the range 15 nm–60 nm. *Journal of Nanoscience and Nanotechnology* 2011, 11 (2), 1141–1146 DOI: 10.1166/jnn.2011.3090.
5. Ghosh, D.; Girigoswami, A.; Chattopadhyay, N. *Journal of Photochemistry and Photobiology A: Chemistry* 2012, 242, 44-50.
6. Hlapisi, N.; Motaung, T. E.; Linganiso, L. Z.; Oluwafemi, O. S.; Songca, S. P. Encapsulation of Gold Nanorods with Porphyrins for the Potential Treatment of Cancer and Bacterial Diseases: A Critical Review. *Bioinorganic Chemistry and Applications* 2019, 2019, 1–27.
7. Lottspeich, F.; Engels, J. W. *Bioanalytics: Analytical methods and concepts in biochemistry and molecular biology*; Wiley-VCH Verlag GmbH & Co. KGaA, 2018.

8. Milestones in cancer research and Discovery:  
<https://www.cancer.gov/research/progress/250-years-milestones>.
9. Norouzi, H.; Khoshgard, K.; Akbarzadeh, F. In vitro outlook of gold nanoparticles in photo-thermal therapy: A literature review. *Lasers in Medical Science* 2018, 33 (4), 917–926 DOI: 10.1007/s10103-018-2467-z.
10. Pivetta, T. P.; Botteon, C. E.; Ribeiro, P. A.; Marcato, P. D.; Raposo, M. Nanoparticle Systems for Cancer Phototherapy: An Overview. *Nanomaterials* 2021, 11 (11), 3132.
11. Shibu, E. S.; Hamada, M.; Murase, N.; Biju, V. Nanomaterials Formulations for Photothermal and Photodynamic Therapy of Cancer. *Journal of Photochemistry and Photobiology C: Photochemistry Reviews* 2012, 15, 53–72.
12. Tarpani, L.; Latterini, L. Plasmonic Effects of Gold Colloids on the Fluorescence Behavior of Dye-Doped SiO<sub>2</sub> Nanoparticles. *Journal of Luminescence* 2017, 185, 192–199.
13. Thakur, N. S.; Bhaumik, J.; Kirar, S.; Banerjee, U. C. Development of Gold-Based Phototheranostic Nanoagents through a Bioinspired Route and Their Applications in Photodynamic Therapy. *ACS Sustainable Chemistry & Engineering* 2017, 5 (9), 7950–7960.
14. Xiang, J.-F.; Liu, Y.-X.; Sun, D.; Zhang, S.-J.; Fu, Y.-L.; Zhang, X.-H.; Wang, L.-Y. Synthesis, Spectral Properties of Rhodanine Complex Merocyanine Dyes as Well as Their Effect on K562 Leukemia Cells. *Dyes and Pigments* 2011, 93 (1-3), 1481–1487.
15. Zengin, G.; Gschneidtnr, T.; Verre, R.; Shao, L.; Antosiewicz, T. J.; Moth-Poulsen, K.; Käll, M.; Shegai, T. Evaluating Conditions for Strong Coupling between

- Nanoparticle Plasmons and Organic Dyes Using Scattering and Absorption Spectroscopy. *The Journal of Physical Chemistry C* 2016, 120 (37), 20588–20596.
16. Zou, J.; Li, L.; Yang, Z.; Chen, X. Phototherapy Meets Immunotherapy: A Win–Win Strategy to Fight against Cancer. *Nanophotonics* **2021**, *10*, 3229–3245.